Structural Engineering and Mechanics, Vol. 21, No. 1 (2005) 101-119 101
DOI: http://dx.doi.org/10.12989/sem.2005.21.1.101

Seismic evaluation of fluid-elevated tank-foundation/soil systems in frequency domain

R. Livaoglu† and A. Dogangun‡

Karadeniz Technical University, Department of Civil Engineering, 61080, Trabzon, Turkey

(Received October 8, 2004, Accepted May 24, 2005)

Abstract. An efficient methodology is presented to evaluate the seismic behavior of a Fluid-Elevated Tank-Foundation/Soil system taking the embedment effects into accounts. The frequency-dependent cone model is used for considering the elevated tank-foundation/soil interaction and the equivalent spring-mass model given in the Eurocode-8 is used for fluid-elevated tank interaction. Both models are combined to obtain the seismic response of the systems considering the sloshing effects of the fluid and frequency-dependent properties of soil. The analysis is carried out in the frequency domain with a modal analysis procedure. The presented methodology with less computational efforts takes account of; the soil and fluid interactions, the material and radiation damping effects of the elastic half-space, and the embedment effects. Some conclusions may be summarized as follows; the sloshing response is not practically affected by the change of properties in stiff soil such as S1 and S2 and embedment but affected in soft soil. On the other hand, these responses are not affected by embedment in stiff soils but affected in soft soils.

Key words: fluid-structure-foundation/soil interaction; elevated tanks; freqency domain analaysis.

1. Introduction

The water supply is essential to control the fires that usually occur during earthquakes, which cause a great deal of damage and loss of life. Therefore, the elevated tanks should remain functional in the post-earthquake period to ensure water supply in earthquake-affected regions. However, several elevated tanks were damaged or collapsed during the past earthquakes. Although this type of structures and their reliability against failure under seismic load are of critical concern, upsetting experiences were shown by the damage to the staging of elevated tank in some earthquakes occurred in different regions of the World (Haroun and Ellaithy 1985). That is why, the seismic behavior of the elevated tanks should be well known, furthermore, they must be designed to be earthquake resistant.

As known, all structures are affected by the soil-structure interaction with varying emphasis on the earthquake excitation. This interaction should be considered for the structures with large slenderness and heavy mass. Moreover, if the structure is an elevated tank, the fluid-structure interaction effects should be considered, as well.

There have been numerous studies done for the dynamic behavior of the fluid storage tanks and

† Doctor, Corresponding author, E-mail: rliva@ktu.edu.tr
‡ Associate Professor

most of them have a connection with the ground level cylindrical tanks. Contrary to this circumstance, very few studies are related to both the underground and the elevated tanks. It is generally assumed that the elevated tanks are fixed to the ground. Therefore, concentration is focused on the dynamic behavior of the fluid and/or the supporting structure. How the subsoil affects the dynamic behavior of the elevated tanks has not been generally discussed in these studies. Almost all existing studies about this subject for the elevated tanks are summarized as follows:

Haroun and Ellaithy (1985) developed a model including an analysis of a variety of elevated rigid tanks undergoing translation and rotation. The model considers fluid sloshing modes; and it assesses the effect of tank wall flexibility on the earthquake response of the elevated tanks. Resheidat and Sunna (1986) investigated the behavior of a rectangular elevated tank considering the soil-foundation-structure interaction during earthquakes. They neglected the sloshing effects on the seismic behavior of the elevated tanks and the radiation damping effect of soil. Haroun and Temraz (1992) analyzed models of two-dimensional X-braced elevated tanks supported on the isolated footings to investigate the effects of the dynamic interaction between the tower and the supporting soil-foundation system but they neglected the sloshing effects. As seen from the studies mentioned above, very few studies have been carried out on the soil-structure interaction effects for the elevated tanks and the frequency-dependent soil properties have not been considered in these studies. Therefore, it is necessary that new studies relevant to the fluid-structure-foundation/soil interaction for the elevated tanks should be carried out by using the frequency-dependent cone method. The main purpose of this study is to investigate the seismic response of the elevated tanks using new approaches for the fluid-structure and soil-structure interactions. The problem investigated for the dynamic fluid-elevated tank-soil interaction can be seen in Fig. 1. A spring-mass model given in the Eurocode-8 is used for the fluid-structure interaction. It considers sloshing effects. The frequency-dependent cone model is used for soil-structure interaction. It considers the radiation damping effects, the embedment effects and the incompressible soil effects.

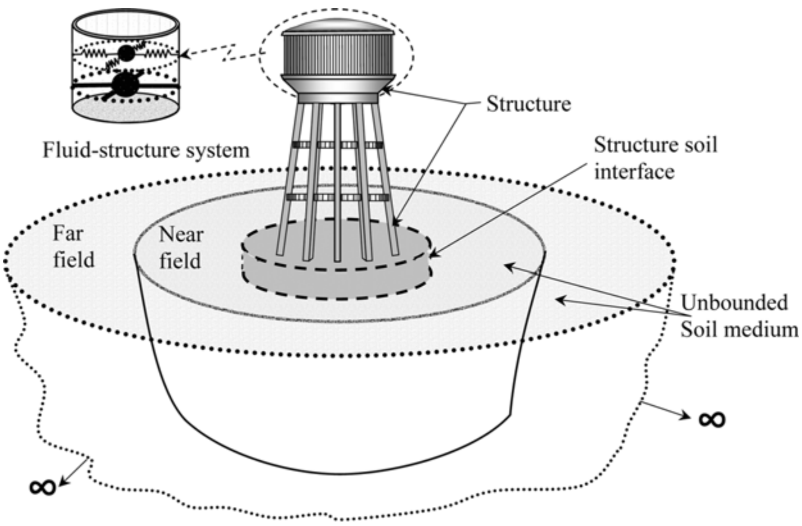

Fig. 1 The problem investigated for dynamic fluid-structure-soil interaction

2. Spring-mass model for fluid-structure interaction

The equivalent spring-mass models have been proposed by some researchers considering the dynamic behavior of the fluid inside a container as shown in Fig. 2. Housner (1963) suggested that an equivalent impulsive mass and a convective mass should represent the dynamic behavior of the fluid as an approximation of the two mass model. The other researchers like Bauer (1964) and Veletsos with co-workers (1984) proposed similar methods including additional higher modes of the convective masses. Then, a more simplified approach has been elaborated by Malhotra *et al.* (2000). This spring-mass model has been used by Eurocode 8 (2003). To the literature, although only the first convective mass may be considered (Housner 1963), additional higher-modes of convective masses may also be included (Chen and Barber 1976, Bauer 1964) in the ground supported tanks. A single convective mass is generally used for practical design of the elevated tanks (Haroun and Housner 1981) and the higher modes of the sloshing have negligible influence on the forces exerted on the container even if the fundamental frequency of the structure is in the vicinity of one of the natural frequencies of the sloshing (Haroun and Ellaithy 1985). As practical analysis is presented in this study, only one convective mass is considered in the numerical example.

Housner (1963) has suggested a simplified analysis procedure for the fixed-base elevated tanks (Fig. 3). In this approach, two masses (m_1 and m_2) are assumed uncoupled and the earthquake forces on the support are estimated by considering two separate single-degree-of-freedom systems. The mass of m_1 represents only the sloshing of the convective mass (m_c), the mass of m_2 consists of the impulsive mass of the fluid (m_i), the mass derived by the weight of the container (m_v) and by some parts of the self-weight of the supporting structure (m_{ss}; two-thirds of the supporting structure

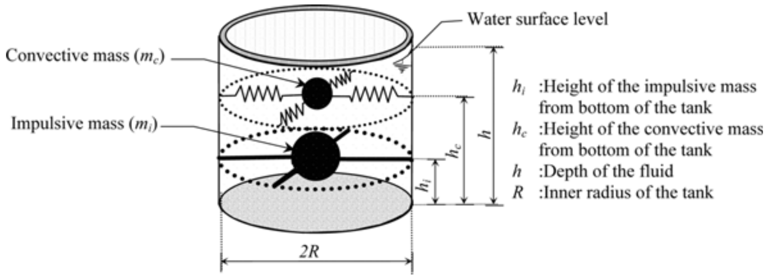

Fig. 2 The equivalent spring-mass model of the fluid

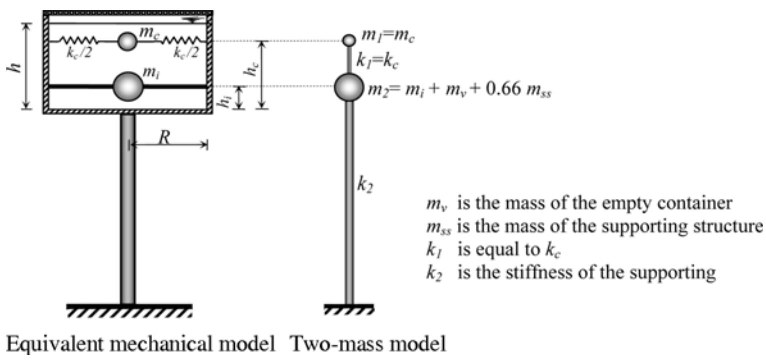

Fig. 3 The two-mass model for the elevated tanks

Table 1 Recommended design values for the impulsive mode and first convective mode of vibration as a function of the tank height-to-radius ratio (*h/R*) (EC-8, 2003)

h/R	C_i	C_c	m_i/m_w	m_c/m_w	h_i/h	h_c/h	h_i'/h	h_c'/h
0.3	9.28	2.09	0.176	0.824	0.400	0.521	2.640	3.414
0.5	7.74	1.74	0.300	0.700	0.400	0.543	1.460	1.517
0.7	6.97	1.60	0.414	0.586	0.401	0.571	1.009	1.011
1.0	6.36	1.52	0.548	0.452	0.419	0.616	0.721	0.785
1.5	6.06	1.48	0.686	0.314	0.439	0.690	0.555	0.734
2.0	6.21	1.48	0.763	0.237	0.448	0.751	0.500	0.764
2.5	6.56	1.48	0.810	0.190	0.452	0.794	0.480	0.796
3.0	7.03	1.48	0.842	0.158	0.453	0.825	0.472	0.825

weight is recommended in ACI 371R (1998) and the total weight of it is by Priestley *et al.* (1986)).

The dynamic characteristics of the elevated tanks in the Eurocode-8 model may be determined by using the expressions and equivalent masses, and their heights from the container bottom given in Table 1. In this table, m_w is the total mass of the fluid, h_i' and h_c' are the heights used instead of h_i and h_c to express the overturning moment immediately below the base plate.

According to this procedure, the natural period T_i for the impulse response and that T_c for the convective response are

$$T_i = C_i \frac{h\sqrt{\rho}}{\sqrt{s/R}\sqrt{E}} \tag{1}$$

$$T_c = C_c\sqrt{R} \tag{2}$$

Where s is the equivalent uniform thickness of the tank wall, ρ is the mass density of the fluid, and E is the Young's modulus of the elasticity of the tank material. The coefficients C_i and C_c may be obtained from Table 1. The coefficient C_i is dimensionless, while C_c is expressed in s/m$^{1/2}$. For tanks with nonuniform wall thickness, s may be computed by taking a weighted average over the wetted height of the container wall (Molhotra 2000), assigning highest weight to the thickness near the base of the container where the strain is maximum value.

The impulsive mass is attached to tank walls by rigid links, whereas the convective mass is connected by springs. A two-mass model was developed by using these equivalent masses and springs. In this model, walls are assumed as rigid and the rigidity of the supporting structure is characterized by k_2 which equals to that of the supporting structure for a horizontal force applied at the same height as the mass. The sloshing frequency ω_c and the stiffness k_1 (or k_c) of a cylindrical tank are given by;

$$\omega_c^2 = \frac{g}{R}1.84\text{th}\frac{1.84 \cdot h}{R}; \quad k_1 = k_c = m_c\omega_c^2 \tag{3}$$

where, g is the ground acceleration.

3. Soil-structure interaction

In the dynamic soil-structure-interaction analysis, a bounded structure (which may be linear or nonlinear), consisting of the actual structure and an adjacent irregular near field soil, will interact with the unbounded (infinite or semi-infinite) far field soil, assumed to be linear elastic.

There are different ways to consider the soil-structure interaction. First of them is the modifying method that can be constructed by modifying the fixed base solution of the structural system (Veletsos and Meek 1974). This method has been widely used in the studies (Aviles and Suarez 2001) and the codes such as ATC-1978 (Veletsos etc. 1988), FEMA 368-369 (2001), and Eurocode-8 (2003). To represent the property of the elastic or viscoelastic half-space accurately, the spring and dashpots are required to depend on the frequency of excitation (Wu and Smith 1995). The second one is the substructure method that can consider the frequency-dependent or independent dynamic stiffness and the damping of the soil/foundation system. If the frequency-dependent dynamic stiffness or the damping is required to be considered, the governing equation for the structure-foundation system is expressed and solved in the frequency domain using Fourier or Laplace transformation (Wu and Smith 1995, Aviles and Perez-Rocha 1998, Takewaki 2003). The third one is the direct method. Here, finite element and boundary element methods or a mixture of these are used in the time or frequency domain (Wolf and Song 1996a, 1996b, Wolf 2003).

The most striking feature in an unbounded soil is the radiation of energy towards infinity, leading to so-called radiation damping even in a linear system. Mathematically, in a frequency-domain analysis, the dynamic stiffness relating the amplitudes of the displacements to those of the interaction forces in the nodes of the structure-soil interface of the unbounded soil is a complex function. This occurs when the unbounded soil consists of a homogeneous half-space (Wolf 2002). Therefore, Wolf and Meek (1992, 1993) have proposed a cone model, an example of the substructure method, for evaluating the dynamic stiffness and the effective input motion of a foundation on the ground. Wolf and Preisig (2003) adopted this method for the layered half-space. Compared to more rigorous numerical methods, this cone model requires only a simple numerical manipulation within reasonable accuracy (Wolf 1994, Takewaki 2003).

Simple physical models representing the unbounded soil can be applied as follows: the effect of the interaction of the soil and the structure on the response of the latter would be negligible in some cases and need not to be considered in the other cases. This is applied, for example, to a flexible high-rise structure with a small mass where the influence of the higher modes on the seismic response remains small. Exciting the base of the structure with the prescribed earthquake motion is then possible. For load applied directly to the structure, the soil can be represented by a static spring or the structure can even be regarded as built-in (Wolf 1994, 2002). These static stiffnesses are expressed in the literature with different theory. From all, the Boussinesq theory can be summarized as follows: when a homogeneous halfspace is statically loaded, the variations of displacements with the increasing depth are assumed as in Fig. 4. The shape is also like a truncated cone, for the dynamic loading. Static stiffness of this truncated cone in a circular rigid foundation can be expressed as in Table 2.

In the above table K_v, K_H, K_R and K_T are the vertical, horizontal, rocking and torsional stiffnesses of a circular foundation, respectively. For other geometrical shapes, these are given for square and rectangular shapes by Wolf (1994) and for other arbitrary shape by Dobry and Gazetas (1986) and Gazetas and Tassoulas (1987). Since the stiffness is frequency-dependent in the dynamic loading, these static stiffnesses are used for calculating the dynamic stiffness $[S(a_0)]$ estimated by the

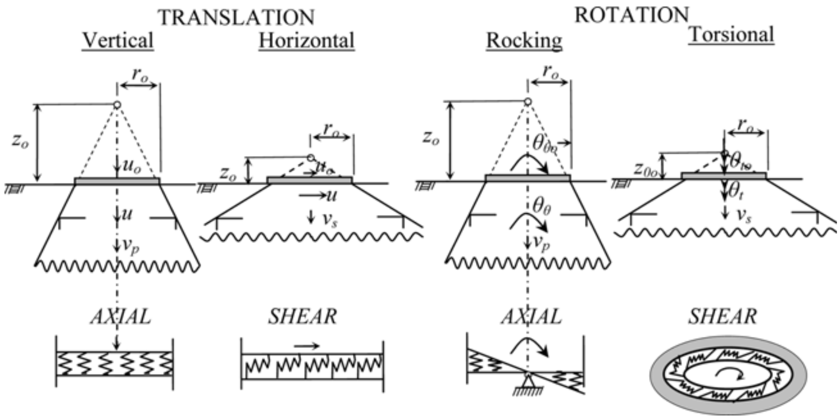

Fig. 4 Cones for various degrees-of-freedom with corresponding aspect ratio (z_o/r_o), wave-propagation velocity and distortion (Wolf 1994), v_s and v_p are the shear and dilatational wave velocities

Table 2 Static stiffness values of rigid circular foundation, G: shear modulus, r_0: radius of a circular foundation, υ: Poisson ratio, e: embedment height

Stiffness	Foundation with no embedment	Foundation with embedment
Vertical (K_v)	$\frac{4Gr_o}{1-\upsilon}$	$\frac{4Gr_o}{1-\upsilon}\left(1+0.54\frac{e}{r_o}\right)\left(1+\left(0.85-0.28\frac{e}{r_o}\right)\right)$
Horizontal (K_H)	$\frac{8Gr_o}{2-\upsilon}$	$\frac{8Gr_o}{2-\upsilon}\left(1+\frac{e}{r_o}\right)$
Rocking (K_R)	$\frac{8Gr_o^3}{3(1-\upsilon)}$	$\frac{8Gr_o^3}{3(1-\upsilon)}\left[1+2.3\frac{e}{r_o}+0.58\left(\frac{e}{r_o}\right)^3\right]$
Torsional (K_T)	$\frac{16Gr_o^3}{3}$	$\frac{16Gr_o^3}{3}\left(1+2.67\frac{e}{r_o}\right)$

following equation:

$$S(a_0) = K(k(a_0) + ia_0c(a_0)) \tag{4}$$

Where $k(a_0)$ is the dynamic spring coefficient, $c(a_0)$ is the dynamic damping coefficient (including radiation damping) and a_0 is the dimensionless frequency which equals $\omega r_0/v_s$ where ω is the excitation frequency.

The dynamic coefficients [$k(a_0)$, $c(a_0)$] of the translational cone and [$k_\theta(a_0)$, $c_\theta(a_0)$] of the rotational cone for a rigid foundation resting on the surface of halfspace could be estimated using Eqs. (5) and (6), respectively.

$$k(a_0) = 1 - \frac{\mu z_0 v_s^2}{\pi r_0 v^2}a_0^2, \qquad c(a_0) = \frac{z_0 v_s}{r_0 v} \tag{5}$$

$$k_\theta(a_0) = 1 - \frac{4}{3}\frac{\mu_\theta z_0 v_s^2}{\pi r_0 v^2}a_0^2 - \frac{1}{3}\frac{a_0^2}{\left(\frac{r_0 v}{z_0 v_s}\right)^2 + a_0^2} \qquad c_\theta(a_0) = \frac{z_0 v_s}{3 r_0 v}\frac{a_0^2}{\left(\frac{r_0 v}{z_0 v_s}\right)^2 + a_0^2} \tag{6}$$

For the horizontal motion, a truncated cone moves with the shear wave velocity ($v = v_s$) and the aspect ratio (z_0/r_0) of the cone is equal to $(2 - \upsilon)\pi/8$. In this circumstance μ is zero for all values of Poisson ratios (υ). For the vertical motion, truncated cone moves with dilatational wave velocity (v_p) and $\mu_\theta = 0$ for $\upsilon \le 1/3$. The velocity of the truncated cone is $v = 2v_s$ and the aspect ratio (z_0/r_0) is equal to $(1 - \upsilon)(v/v_s)^2\pi/4$ for $1/3 < \upsilon \le 1/2$ interval. Trapped mass for this interval can be estimated by using Eq. (7) and Eq. (8).

Similar to the horizontal motion, the truncated cone moves with the shear wave velocity ($v = v_s$) for the torsional motion and the aspect ratio of the cone is equal to $9\pi/32$. The value of μ is zero for all values of Poisson ratios under this circumstance. For the rocking motion, the truncated cone velocity is equal to v_p, $\mu_\theta = 0$ for $\upsilon \le 1/3$. The truncated cone moves with $v = 2v_s$ and the aspect ratio is equal to $(1 - \upsilon)(v/v_s)^2 9\pi/32$ for $1/3 < \upsilon \le 1/2$ and the trapped mass for this Poisson ratio interval can be estimated using Eq. (9) and Eq. (10). It should be noted that for $1/3 < \upsilon \le 1/2$, soil is nearly incompressible. This behavior corresponds to trapped soil beneath the foundation, which moves as a rigid body in phase with the foundation. A close match is achieved by defining the trapped mass (ΔM) to be

$$\Delta M = \mu \rho r_0^3 \tag{7}$$

where

$$\mu = 2,4\pi\left(\upsilon - \frac{1}{3}\right) \tag{8}$$

for the vertical motion and the trapped mass moment of inertia (ΔM_θ)

$$\Delta M_\theta = \mu_\theta \rho r_0^5 \tag{9}$$

where

$$\mu_\theta = 0,3\pi\left(\upsilon - \frac{1}{3}\right) \tag{10}$$

for the rocking motion. In the intermediate and higher frequency ranges, the dynamic stiffness coefficient is governed by the damping coefficient, as $c(a_0)$ is multiplied by a_0 in contrast to $k(a_0)$. Both $c_v(a_0)$ and $c_H(a_0)$ of the cone model produce very accurate results in this frequency ranges (Wolf 1994). Whereas in the lower-frequency range ($a_0 < 2$) and for $\upsilon \le 1/3$, which is of practical importance, the cone's results overestimate (radiation) damping to certain extent, especially in the vertical motion (Wolf 1994).

4. Practical procedure for the systems including embedment and incompressible soil effects

Initially, to determine all the system response to the dynamic excitation, the system must be

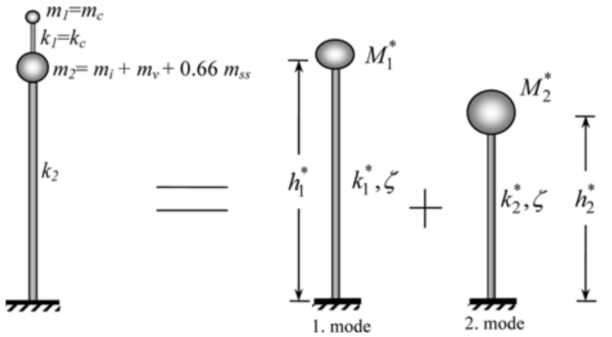

Fig. 5 Two mass model represented by two mode properties of the elevated tank

represented by four properties (Fig. 3). First one is lateral stiffness of the supporting structure (k_2). This stiffness of the typical staging system with basic configuration (see Fig. 7) is estimated using the Eq. (11) suggested by Dutta and co-workers (2000). The second property is the stiffness k_1 for the convective mass given in Eurocode-8 and this is calculated by Eq. (3). The third one is the mass m_1 which is equal to convective mass m_c estimated from Table 1. Finally, the fourth one is the mass m_2 which is summation of the impulse mass (from Table 1), the total mass of the vessel and 66 percent of the mass of the staging system.

$$k_2 = \frac{12 \cdot E_{cl} \cdot I_{cl} \cdot N_{cl}}{h_{cl}^3} \left[\frac{1}{\frac{2 \cdot I_{cl} N_p (4N_p^2 - 1)}{A_c R_s^2} + N_p + 2(N_p - 1)\frac{E_{cl} I_{cl}/h_{cl}}{E_b I_b / L}} \right] \tag{11}$$

Where: E_{cl}, h_{cl}, I_{cl} and N_{cl} are Young's modulus of column material, net height, moment of inertia and the number of the columns, respectively; E_b, L and I_b are Young's modulus of beam material, span and moment of inertia of the beam, respectively; N_p is the number of panels and R_s is the staging radius.

Modal properties like effective modal mass, heights and stiffness can be calculated from this two degree-of-freedom system (Fig. 5).

Where, $M_1^* \& M_2^*$; $h_1^* \& h_2^*$; $k_1^* \& k_2^*$ are the efffecive masses, effective heights and effective stiffnesses of the first and the second modes, respectively. These modal properties can be estimated with Eq. (12) and Eq. (13) (Chopra 2000)

$$M_n^* = \Gamma_n L_n^h = \frac{(L_n^h)^2}{M_n}; \quad h_n^* = \frac{L_n^\theta}{L_n^h}; \quad k_n^* = \omega_n^2 M_n^* \tag{12}$$

where

$$M_n = \phi_n^t M \phi_n = \sum_{i=1}^{N} m_i \phi_{jn}^2 \quad : \quad \Gamma_n = \frac{L_n^h}{M_n} \quad : \quad L_n^h = \sum_{i=1}^{N} m_i \phi_{jn} \quad : \quad L_n^\theta = \sum_{i=1}^{N} h_i m_i \phi_{jn} \tag{13}$$

Additionally, N is the total mode number which is considered, ϕ_n is the mode vector of the nth mode and ω_n^2 is the eigenvalue of the nth mode. Thus the elevated tank model can be represented

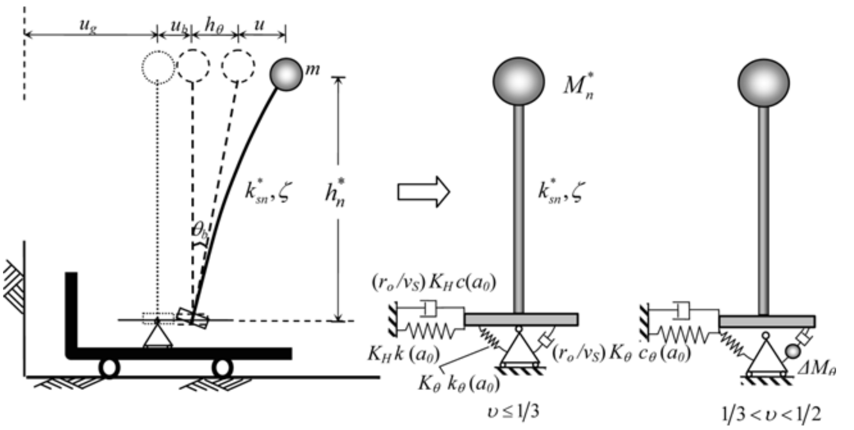

Fig. 6 Dynamic model of structure and soil for horizontal and rocking motions

with two single-degree-of-freedom systems. Because of the absolute differences between the sloshing stiffness k_c and the stiffness of the supporting system k_2, it should be assumed that the first mode represents the sloshing and the second one is concerned with the impulsive mode.

The behavior of single-degree-of-freedom system mentioned above has to be separately calculated in case of soil Poisson ratio for soil $(\upsilon \le 1/3)$ and $(1/3 < \upsilon \le 1/2)$. Because, the trapped or additional mass (ΔM) must be considered in case of $1/3 < \upsilon \le 1/2$ (Fig. 6). Since, more important motions for this type of structures except some special circumstances are the horizontal and the rocking, this type of motion has to be considered for analyzing the fluid-elevated tank-foundation/ soil systems. Then the calculated internal forces or displacement can be combined with any one of the modal combination techniques i.e., ABS, SRSS, CQC etc. (Chopra 2000).

For the system given in Fig. 6, the force-displacement relationship in the horizontal direction and the moment-rotation relationship in the rocking interaction are formulated in frequency domain as

$$P_0(\omega) = K_H k_{H\zeta_g}(a_0)u_0(\omega) + \frac{r_0}{v_s}K_H c_{H\zeta_g}(a_0)\dot{u}_0(\omega) = S_{H\zeta_g}(a_0)u_b(\omega) \tag{14}$$

$$M_0(\omega) = K_\theta k_{\theta\zeta_g}(a_0)\theta_b(\omega) + \frac{r_0}{v_s}K_\theta c_{\theta\zeta_g}(a_0)\dot{\theta}_b(\omega) = S_{\theta\zeta_g}(a_0)\theta_b(\omega) \tag{15}$$

where, $k_{H\zeta_g}, c_{H\zeta_g}, k_{\theta\zeta_g}$ and $c_{\theta\zeta_g}$ are the dynamic stiffness coefficients including ground damping effects of the circular foundation/soil system. The dynamic stiffnesses $[(S_{H\zeta_g}(a_0))$ and $(S_{\theta\zeta_g}(a_0))]$ for the horizontal and rocking motions depending on the dimensionless frequency are approximated as below;

$$S_{H\zeta_g}(a_0) = K_H k_{H\zeta_g}(a_0)(1 + 2i\zeta_H(a_0) + 2i\zeta_g) \tag{16}$$

$$S_{\theta\zeta_g}(a_0) = K_\theta k_{\theta\zeta_g}(a_0)(1 + 2i\zeta_\theta(a_0) + 2i\zeta_g) \tag{17}$$

where ζ_g is the material damping ratio of the soil, $\zeta_H(a_0)$ and $\zeta_\theta(a_0)$ are the radiation-damping ratios for the horizontal and rocking motion of the soil to be estimated as;

$$\zeta_H(a_0) = \frac{a_0 c_H(a_0)}{2k_H(a_0)}, \quad \zeta_\theta(a_0) = \frac{a_0 c_\theta(a_0)}{2k_\theta(a_0)} \tag{18}$$

For a system of three-degrees-of-freedom, the dynamic equilibrium can be formulated for $\upsilon \leq 1/3$ as:

$$-M_n^*\omega^2[u(\omega) + u_b(\omega) + h\theta_b(\omega)] + k_n^*(1+2i\zeta)u(\omega) = M_n^*\omega^2 u_g(\omega) \tag{19}$$

$$-M_n^*\omega^2[u(\omega) + u_b(\omega) + h\theta_b(\omega)] + S_{H\zeta_g}(a_0)u_b(\omega) = M_n^*\omega^2 u_g(\omega) \tag{20}$$

$$-M_n^*h\omega^2[u(\omega) + u_b(\omega) + h\theta_b(\omega)] + S_{\theta\zeta_g}(a_0)\theta_b(\omega) = M_n^*h\omega^2 u_g(\omega) \tag{21}$$

Eqs. (19), (20) and (21) can be written with some elimination as below:

$$\begin{bmatrix} \frac{\omega_{sn}^2}{\omega^2}(1+2i\zeta) - 1 & -1 & -1 \\ -1 & \frac{S_{H\zeta_g}(a_0)}{M_n^*\omega^2} - 1 & -1 \\ -1 & -1 & \frac{S_{\vartheta\zeta_g}(a_0)}{M_n^*h^2\omega^2} - 1 \end{bmatrix} \begin{Bmatrix} u(\omega) \\ u_b(\omega) \\ h\theta_b(\omega) \end{Bmatrix} = \begin{Bmatrix} 1 \\ 1 \\ 1 \end{Bmatrix} u_g(\omega) \tag{22}$$

where $u_b(\omega)$ and $h\theta_b(\omega)$ are expressed using $u(\omega)$ as;

$$u_b(\omega) = \frac{\omega_{sn}^2(1+2i\zeta)}{\frac{S_{H\zeta_g}(a_0)}{M_n^*}}u(\omega) \qquad h_n^*\theta_b(\omega) = \frac{\omega_{sn}^2(1+2i\zeta)}{\frac{S_{\theta\zeta_g}(a_0)}{M_n^*h_n^{*2}}}u(\omega) \tag{23}$$

Eqs. (22) and (23) yield the following equation:

$$u(\omega) = \frac{1}{\left[\frac{1}{\omega^2} - \frac{M_n^*}{S_{H\zeta_g}(a_0)} - \frac{\omega^2 M_n^* h_n^{*2}}{S_{\theta\zeta_g}(a_0)} - \frac{1}{\omega_{sn}^2(1+2i\zeta)}\right](1+2i\zeta)\omega_{sn}^2} u_g(\omega) \tag{24}$$

If the same equations were written for $1/3 < \upsilon \leq 1/2$, Eq. (22) could be written as

$$\begin{bmatrix} \frac{\omega_{sn}^2}{\omega^2}(1+2i\zeta) - 1 & -1 & -1 \\ -1 & \frac{S_{H\zeta_g}(a_0)}{M_n^*\omega^2} - 1 & -1 \\ -1 & -1 & \frac{S_{\vartheta\zeta_g}(a_0)}{M_n^*h^2\omega^2} - \frac{\Delta M_\theta}{M_n^*h^2} - 1 \end{bmatrix} \begin{Bmatrix} u(\omega) \\ u_b(\omega) \\ h\theta_b(\omega) \end{Bmatrix} = \begin{Bmatrix} 1 \\ 1 \\ 1 \end{Bmatrix} u_g(\omega) \tag{25}$$

where $u_b(\omega)$ and $h\theta_b(\omega)$ are expressed using $u(\omega)$ as;

$$u_b(\omega) = \frac{\omega_{sn}^2(1+2i\zeta)}{\frac{S_{H\zeta_g}(a_0)}{M_n^*}}u(\omega) \qquad h_n^*\theta_b(\omega) = \frac{\omega_{sn}^2(1+2i\zeta)}{\frac{S_{\vartheta\zeta_g}(a_0)}{M_n^*h^2} - \frac{\Delta M_\theta}{M_n^*h^2}\omega^2}u(\omega) \tag{26}$$

The lateral displacement depending on the structural rigidity was derived using Eqs. (25) and (26) in the incompressible soil as below:

$$u(\omega) = \frac{u_g(\omega)}{\omega_{sn}^2(1+2i\zeta)\left[\frac{1}{\omega^2} - \frac{1}{\omega_{sn}^2(1+2i\zeta)} - \frac{M_n^*}{S_{H\zeta_g}(a_0)} - \frac{1}{\frac{S_{\vartheta\zeta_g}(a_0)}{M_n^*h^2} - \frac{\Delta M_\theta}{M_n^*h^2}\omega^2}\right]} \tag{27}$$

Where, $\omega_{sn}^2(=k_{sn}^*/M_n^*)$ is the square of the angular frequency of the fixed base single-degree-of-freedom system, $u_g(\omega)$ is the effective input motion in the frequency domain. It may be obtained by means one of the transformation techniques like Fourier and Laplace. i.e., Using Fourier transformation, the displacements in the time domain $u_g(t)$ can be expressed in the frequency domain as;

$$u_g(\omega) = \int_{-\infty}^{\infty} u_g(t)\exp(-i\omega t)dt \tag{28}$$

The solution in the frequency domain can be expressed in the time domain using inverse Fourier transformation like Eq. (29).

$$u(t) = \frac{1}{T}\int_{-\infty}^{\infty} u(\omega)\exp(i\omega t)d\omega \tag{29}$$

5. Numerical example

A reinforced concrete elevated tank with a container capacity of 900 m^3 is considered in seismic analysis (Fig. 7). The elevated tank has a frame supporting structure in which columns are connected by the circumferential beams at regular interval at 7 m and 14 m height level. The tank container is Intze type. The container and the supporting structure have been used as a typical project in Turkey up to recent years. Young's modulus and the weight of concrete per unit volume are taken to be 32,000 MPa and 25 kN/m^3, respectively. The container is filled with the water density of 1,000 kg/m^3. Calculated modal properties are m_t = 1,281,000 kg, m_c = 281,000 kg, k_i = 846,000 N/m, k_2 = 32,900,000 N/m.

In the seismic analysis, it is assumed that the tank is subjected to North-South component of the August 17, 1999 Kocaeli Earthquake in Turkey (Fig. 8). The ground acceleration of North-South component of this earthquake was taken into consideration for approximately forty seconds.

While the damping in the convective mode (the first mode) may be accepted as 0.5%, for the second mode as the impulsive mode accepted as 5% for the reinforced concrete supporting system.

To evaluate variations of the dynamic parameters in the elevated tanks depending on soil

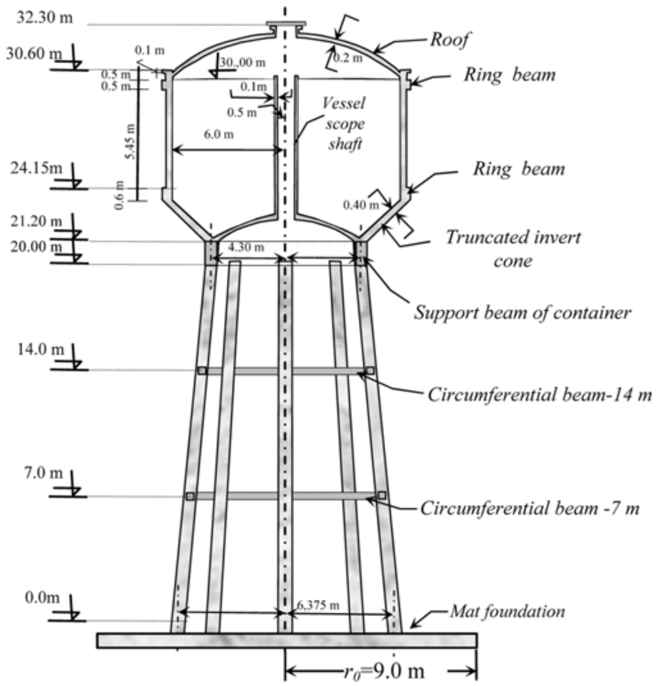

Fig. 7 Vertical cross section of the reinforced concrete elevated tank considered for the seismic analysis

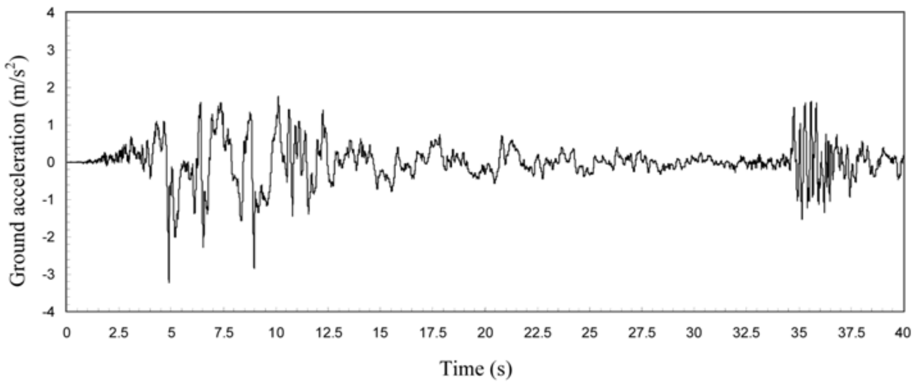

Fig. 8 North-South component of the August 17, 1999 Kocaeli Earthquake in Turkey

conditions, six soil types as shown in Table 3 were considered. Soil conditions recommended in the literature are considered in the selection of soil types and their properties (Bardet 1997, Cudato 2001).

All of the elevated tanks and soil systems defined in Table 2 are analyzed with the given procedures in this paper. For this procedure, the model for two-degrees-of-freedom system given in Fig. 5 and the model for soil-structure system given in Fig. 6 are adopted for a sample-elevated tank. The analysis is carried out using a computer program (SAET 2004) coded for seismic analysis of elevated tanks.

The seismic analysis of the elevated tank and soil systems were carried out in case of no

Table 3 Properties of the considered soil types

Soil types	ζ_g	E (kN/m^2)	G (kN/m^2)	E_c (kN/m^3)	γ (kg/m^3)	υ	v_s (m/s)	v_p (m/s)
S1	5.00	7000000	2692310	9423077	2000	0.30	1149.1	2149.89
S2	5.00	2000000	769230	2692308	2000	0.30	614.25	1149.16
S3	5.00	500000	192310	673077	1900	0.35	309.22	643.68
S4	5.00	150000	57690	201923	1900	0.35	169.36	352.56
S5	5.00	75000	26790	160714	1800	0.40	120.82	295.95
S6	5.00	35000	12500	75000	1800	0.40	82.54	202.18

Table 4 Results obtained from seismic analysis in case of no embedment

Soil types	Maximum sloshing displacement, u_s		Maximum roof displacement, u		Maximum base shear force, V		Maximum overturning base moment, M_o	
	time (s)	value (m)	time	value (m)	time	value (kN)	time (s)	value (kNm)
S1	22.21	1.108	5.38	0.098	4.89	4691.9	4.89	119990
S2	22.21	1.127	6.34	0.116	4.89	4673.3	4.89	119460
S3	22.22	1.153	9.52	0.104	4.89	4594.3	4.89	117210
S4	22.26	1.282	9.60	0.127	4.89	4359.1	4.89	110720
S5	22.33	1.489	9.73	0.148	4.89	4182.6	4.89	106750
S6	20.85	1.812	7.82	0.154	4.89	4579.0	4.89	130290

Table 5 Results obtained from seismic analysis in case of embedment ($e/r_o = 1$)

Soil types	Maximum sloshing displacement, u_s		Maximum roof displacement, u		Maximum base shear force, V		Maximum overturning base moment, M_o	
	time (s)	value (m)	time	value (m)	time	value (kN)	time (s)	value (kNm)
S1	22.21	1.103	5.37	0.094	4.89	4697.6	4.89	120150
S2	22.21	1.107	5.38	0.098	4.89	4692.7	4.89	120010
S3	22.21	1.114	9.50	0.095	4.89	4672.9	4.89	119440
S4	22.22	1.147	9.52	0.103	4.89	4605.3	4.89	117520
S5	22.24	1.192	9.55	0.113	4.89	4510.5	4.89	114850
S6	22.27	1.308	9.63	0.129	4.89	4337.7	4.89	110230

embedment ($e/r_o = 0$) and embedment ($e/r_o = 1$). The obtained peak values and their times for the maximum sloshing displacements, roof displacements, base shear forces and overturning base moments are given in Tables 4 and 5, respectively.

As seen from Tables 4 and 5, the embedment affects the values of seismic structural responses such as the roof displacement, base shear and overturning moment. Its effects on the value of the sloshing displacement is practically negligible. It is generally expected that when soil gets softer, displacements tend to increase and shear forces tend to decrease. As can be realized from Tables 4 and 5, these trends may not satisfy all soil types.

Only peak values may be seen adequately for practically design purposes. However, it is not enough to evaluate all seismic responses of the elevated tanks during an earthquake. Therefore, it will be helpful to give time histories for the responses as below:

5.1 Sloshing displacement

The estimated sloshing displacements varying in time for S1 and S6 were illustrated in Fig. 9. As seen from this figure, a different sloshing response was obtained for different soil types. Maximum displacement reaches 1.108 m in 22.21 s for S1 and 1.812 in 20.85 s for S6. It is seen that approximately the maximum displacement practically occurs at the same time ($t = 21$s~22s). The maximum deviation from S6 to S1 in the sloshing displacement is 64%. Since this circumstance is similar, graphs for other soil types are not given here.

The variations in time of the obtained sloshing displacements for the stiff soil types like S1 and

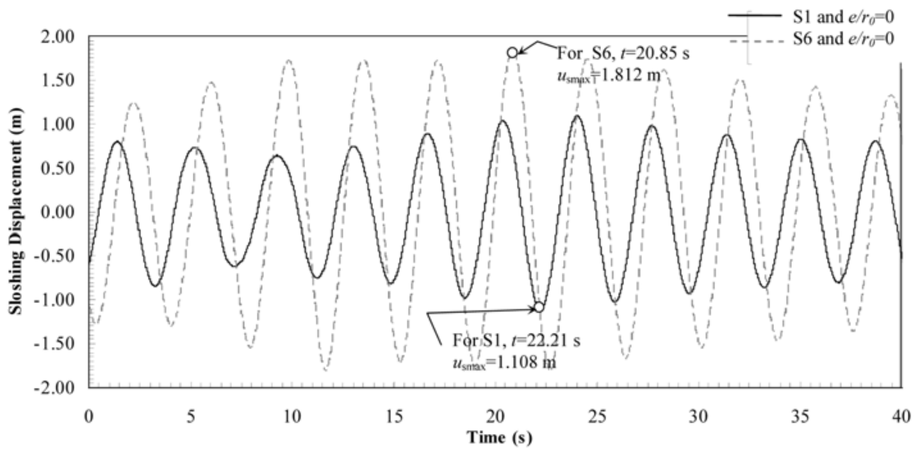

Fig. 9 Variation of the sloshing displacement in time for soil types of S1 and S6, no embedment

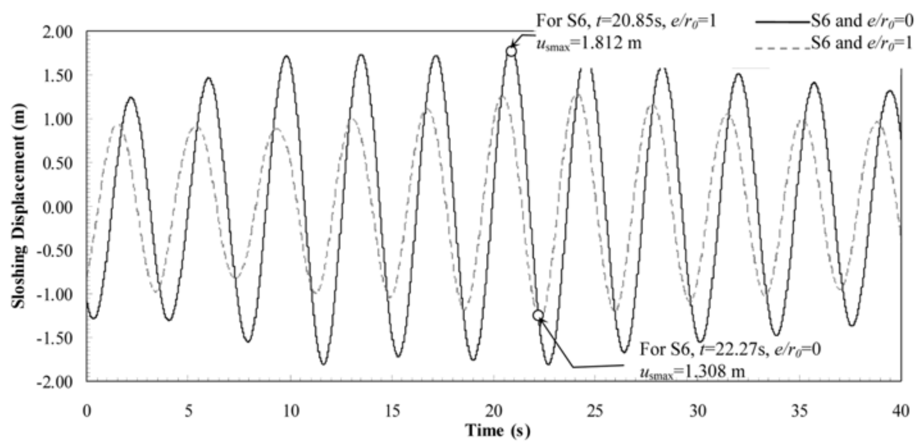

Fig. 10 Variation of the sloshing displacement in time for soil type of S6, no embedment and embedment ($e/r_o = 1$)

S2 are similar. It is said that the sloshing response is not affected by the embedment for these types. To see only the embedment effect on the sloshing response, the sloshing displacements varying in time in case of no embedment and embedment were investigated. As graphs are almost similar in stiff soils, they are not illustrated here. However soil gets softer, different behaviors can be shown as appeared in Fig. 10. Effects of the embedment on the dynamic behavior of the elevated tanks are considerable as to be seen from this figure.

5.2 Roof displacement

The comparative variation of the estimated roof displacements for S1 and S6 is illustrated in Fig. 11. As seen from this figure different roof displacement responses are estimated for different the soil types. i.e., The maximum roof displacement reaches 0.098 m in 5.38 s for S1, 0.104 m in 9.52 s for S4 and 0.154 m in 7.82 s for S6. The maximum deviation in the roof displacement for soil types of S6 to S1 is approximately 57%.

To see only embedment effect on the roof displacement response, the displacement for S1 with no

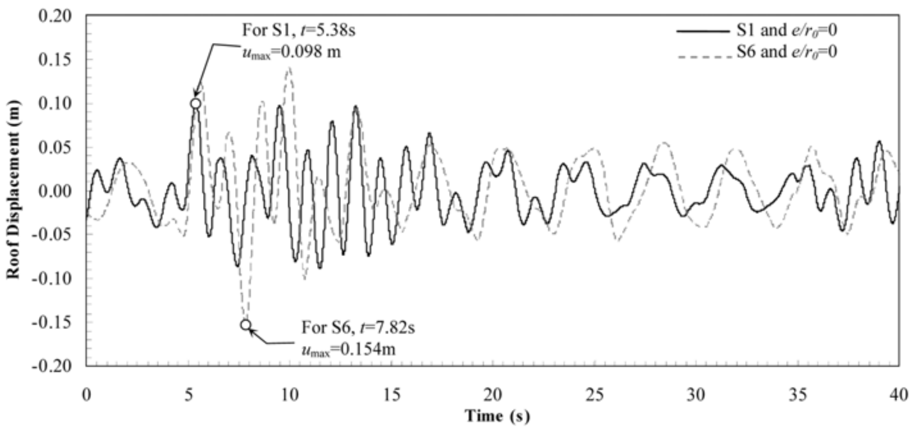

Fig. 11 Variation of the roof displacement in time for soil types of S1 and S6, no embedment

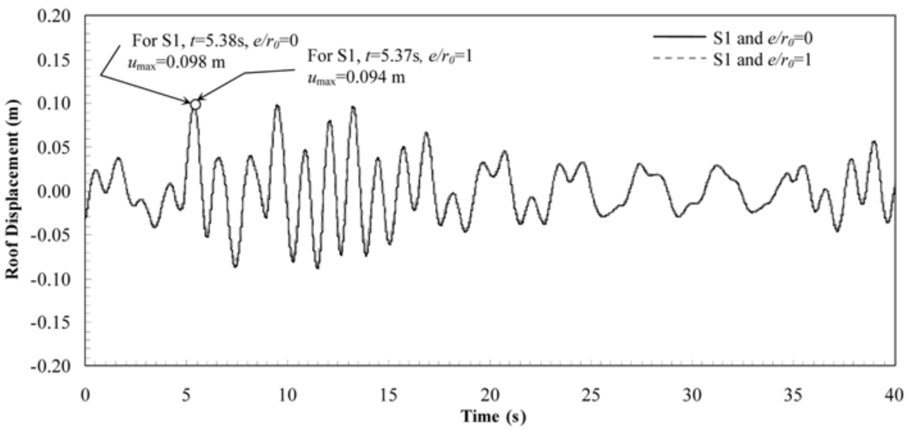

Fig. 12 Variation of the roof displacement in time for soil type of S1, no embedment and embedment ($e/r_o = 1$)

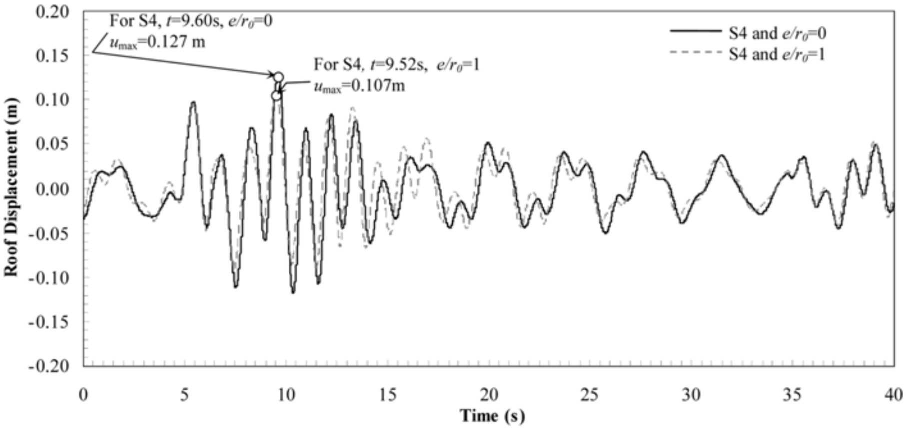

Fig. 13 Variation of the roof displacement in time for soil type of S4, no embedment and embedment ($e/r_o = 1$)

embedment ($e/r_o = 1$) and embedment ($e/r_o = 1$) are illustrated in Figs. 12 and 13, respectively. As seen from these figures, two graphs are approximately similar for S1, but different graphs were obtained for S4. It is said that the roof displacement response is not affected by the embedment in relatively stiff soils (such as S1 and S2) but it is affected by the embedment in relatively soft soils (such as S3-S6).

5.3 Base shear force

The estimated base shear forces for S1 and S6 are illustrated in Fig. 14. As can be seen from Fig. 14 different shear force responses were obtained for different soil types. As known, reasons for these different seismic responses for S1 and S6 occurred due to the reduced foundation/soil rigidity and increased radiation damping for S6. The maximum base shear force occurs in 4.89 s with $V = 4697.4$ kN for S1, in 4.89 s with $V = 4337.7$ kN for S6.

To see only embedment effect on the base shear force response, the base shear for S1 and S6 with no embedment and embedment ($e/r_o = 1$) are illustrated in Figs. 15 and 16, respectively. As seen from these figures, similar to the variation of the roof displacement, two graphs were approximately

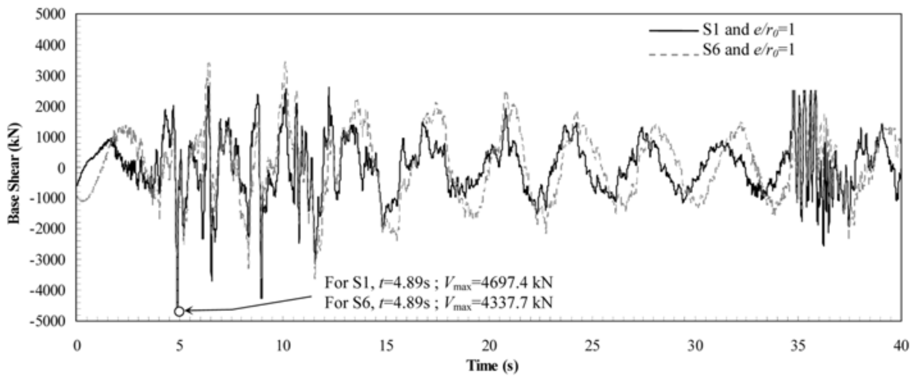

Fig. 14 Variations of the base shear forces in time for soil types of S1 and S6, embedment ($e/r_o = 1$)

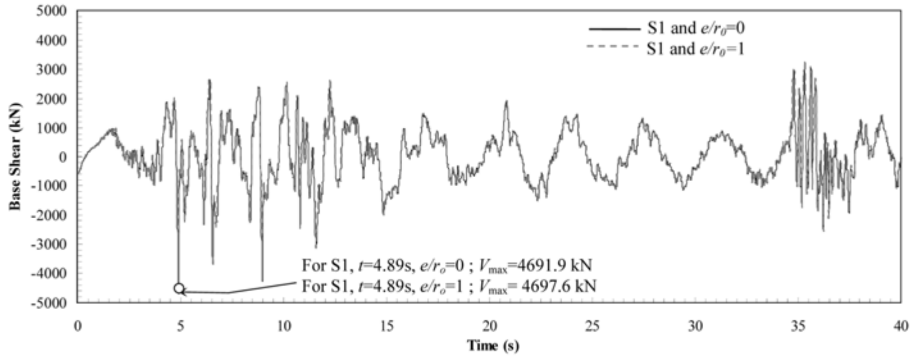

Fig. 15 Variation of the base shear force in time for soil type of S1, no embedment and embedment ($e/r_o = 1$)

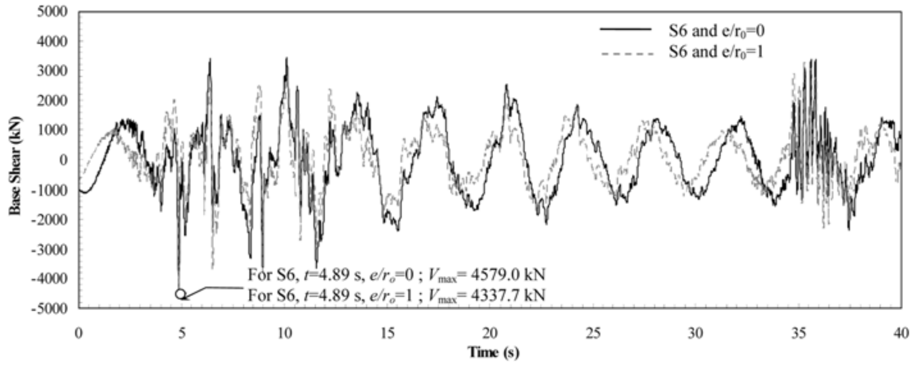

Fig. 16 Variation of the base shear force in time for soil type of S6, no embedment and embedment ($e/r_o = 1$)

same as for S1, but different graphs were obtained for S6. It is said that the base shear force response is not affected by the embedment in relatively stiff soils (such as S1 and S2) but it is affected by the embedment in relatively soft (i.e., S3-S6).

6. Conclusions

A simple procedure is proposed for seismic analysis of fluid-elevated tank-foundation/soil systems. The procedure provides not only an estimation of the base shear, overturning moment and displacement of supporting system but also the sloshing displacement. A computer program was coded for the seismic analysis of the elevated tanks considering interaction effects. Analysis with this procedure needs less computer memory capacity and shorter CPU times.

The sloshing response is not practically affected by soil properties and embedment in stiff soils such as S1, S2. Similarly, roof displacement and base shear force responses are also not affected by the embedment in relatively stiff soils but they are affected by the embedment in relatively soft soils.

Generally, when soil gets softer, the roof displacements increase, the base shear and overturning moment decrease. However, if an earthquake is considered in the analysis, this may lead to wrong assessment of the seismic response. Therefore, to prevent misleading results, time history analyses are necessary in case that soil-structure interaction is not negligible.

It is seen that the results obtained in relatively stiff soils (like S1 and S2) overestimate radiation damping in the lower-frequency range. It should be noted that soil-structure interaction has less importance in such soil conditions.

It is recommended that more numerical examples analyzed for different soil types and foundation conditions. Furthermore, the procedure presented here can be used with other substructure methods.

Acknowledgements

This study constitutes some parts of the first author's doctoral research. We thank to reviewers who gave useful comments on this paper.

References

ACI 371R-98. (1995), American Concrete Institute, "Guide to the analysis design and construction of concrete-pedestal water tower".

Aviles, J. and Perez-Rocha, E.L. (1998), "Effect of foundation embedment during building-soil structure interaction", *Earthq. Eng. Struct. Dyn.*, **27**, 1523-1540.

Aviles, J. and Suarez, M. (2002), "Effective periods and damping of building-foundation systems including seismic wave effects", *Eng. Struct.*, **24**, 553-562.

Bardet, P.J. (1997), *Experimental Soil Mechanics*, Prentice Hall, Upper Saddle River, New Jersey 07458.

Bauer, H.F. (1964), *Fluid Oscillations in the Containers of a Space Vehicle and Their Influence Upon Stability*, NASA TR R-187.

Chen, C.P. and Barber, R.B. (1976), "Seismic design of liquid storage tanks to earthquakes", *Int. Symposium on Earthquake Structural Engineering*, St. Louis Missouri, II: 1231.

Chopra, K.A. (2000), *Dynamics of Structures: Theory and Applications to Earthquake Engineering*, Prentice-Hall International Inc.

Coduto, P.D. (2001), *Foundation Design: Principles and Practices : Second Edition*, Prentice Hall, Upper Saddle River, New Jersey.

Dobry, R. and Gazetas, G. (1986), "Dynamic response of arbitrarily-shaped foundations", *ASCE. Geotechnical Engineering Division. J.*, **113**(2), 109-135.

Dutta, S.C., Jain, S.K. and Murty, C.V.R. (2000), "Assessing the seismic torsional vulnerability of elevated tanks with RC frame-type staging", *Soil Dyn. Earthq. Eng.,* **19**, 183-197.

Eurocode-8. (2003), *Design of Structures for Earthquake Resistance-Part 4 (Draft No:2)*: *Silos, Tanks and Pipelines*, European Committee for Standardization, 65p.

FEMA 368. (2000), *The 2000 NEHRP Recommended Provisions for New Buildings and Other Structures Part 1: Provision*, NEHRP.

FEMA 369. (2000), *The 2000 NEHRP Recommended Provisions for New Buildings and Other Structures Part 2: Commentary*, NEHRP.

Gazetas, G. and Tassoulas, J.L. (1987), "Horizontal stiffness of arbitrarily-shaped embedded foundations", *ASCE. Geotechnical Engineering Division. J.*, **113**(5), 440-457.

Haroun, M.A. and Ellaithy, M.H. (1985), "Seismically induced fluid forces on elevated tanks", *J. Technical Topics in Civil Eng.*, **111**(1), 1-15.

Haroun, M.A. and Temraz, M.K. (1992), "Effects of soil-structure interaction on seismic response of elevated tanks", *Soil Dyn. Earthq. Eng.*, **11**(2), 73-86.

Haroun, M.A. and Housner, G.W. (1981), "Seismic design of liquid storage tanks", *J. Tech. Councils.* ASCE, **107**(1), 191-207.

Housner, G.W. (1963), "Dynamic behavior of water tanks", *Bulletin of the Seismological Society of the America*,

53, 381-387.

Meek, J.W. and Wolf, J.P. (1994), "Cone models for embedded foundation", *J. Geotechnical Eng.*, ASCE, **120**(1), 60-80.

Priestley, M.J.N., Davidson, B.J., Honey, G.D., Hopkins, D.C., Martin, R.J., Ramsey, G., Vessey, J.V. and Wood, J.H. (1986), *Seismic Design of Storage Tanks, Recommendation of a Study Group the New Zealand Society for Earthquake Engineering*, New Zealand.

Resheidat, R.M. and Sunna, H. (1986), "Behavior of elevated storage tanks during earthquakes", *Proc. the 3th U.S. Nat. Conf. on Earthquake Engineering,* 2143-2154.

SAET-2004. (2004), "A computer program for seismic analysis of elevated tanks considering fluid-structure-soil interaction", Karadeniz Technical University.

Takewaki, I., Takeda, N. and Uetani, K. (2003), "Fast practical evaluation of soil-structure interaction of embedded structure", *Soil Dyn. Earthq. Eng.*, **23**, 195-202.

Veletsos, S.A., Prasad, M.A. and Tang, Y. (1988), "Design approaches for soil structure interaction", National Center for Earthquake Engineering Research, Technical Report NCEER-88-00331.

Veletsos, A.S. and Meek, J.M. (1974), "Dynamics of behaviour of building-foundation systems", *Earthq. Eng. Struct. Dyn.*, **3**, 121-138.

Veletsos, A.S. (1984), *Seismic Response and Design of Liquid Storage Tanks, Guidelines for the Seismic Design of Oil and Gas Pipeline Systems.* ASCE, New York, 255-461.

Wolf, J.P. and Song, C.H. (1996a), *Finite-Element Modeling of Unbounded Media*. Chichester: John Wiley & Sons.

Wolf, J.P. and Song, C. (1996), "Consistent infinitesimal finite element cell method - a boundary finite-element procedure", *Third Asian-Pacific Conf. on Computational Mechanics,* Seoul, Korea, 16-18 September 1996.

Wolf, J.P. (1994), *Foundation Vibration Analysis Using Simple Physical Models*, Prentice-Hall, Englewood Cliffs.

Wolf, J.P. (2002), "Some cornerstones of dynamic soil-structure interaction", *Eng. Struct.*, **24**, 13-28.

Wolf, J.P. (2003), "Dynamic stiffness of foundation embedded in layered halfspace based on wave propagating cones", *Earthq. Eng. Struct. Dyn.*, **32**, 1075-1098.

Wolf, J.P. and Meek, J.W. (1993), "Cone models for a soil layer on a flexible rock half-space", *Earthq. Eng. Struct. Dyn.*, **22**, 185-193.

Wolf, J.P. and Meek, J.W. (1992), "Cone models for homogeneous soil", *J. Geotechnical Eng.,* ASCE, **118**, 686-703.

Wolf, J.P. and Preisig, M. (2003), "Dynamic stiffness of foundation embedded in layered halfspace based on wave propagation in cones", *Earthq. Eng. Struct. Dyn.*, **32**, 1075-1098.

Wolf, J.P. (2003), *The Scaled Boundary Element Method,* John Wiley&Sons.

Wu, W. and Smith, A. (1995), "Efficient modal analysis for structures with soil-structure interaction", *Earthq. Eng. Struct. Dyn.*, **24**, 283-289.